RNA sequencing analysis reveals differential gene expression of CXCL2 in ACPA-positive and ACPA-negative rheumatoid arthritis

Lin Sun
Peking University Third Hospital
Xinyu Wang
Peking University Third Hospital
Ning He
Chinese Academy of Sciences
Zhuo An
Peking University Third Hospital
Ruohan Yu
Peking University Third Hospital
Yanming Li
Chinese Acdemy of Sciences
Yongjun Li
Chinese Academy of Sciences
Xiangyuan Liu
Peking University Third Hospital
Xiangdong Fang
Chinese Academy of Sciences
Jinxia Zhao (zhao-jinxia@163.com)
Peking University Third Hospital https://orcid.org/0000-0002-8225-0921

Research article

Keywords: CXCL2, Osteoclast, Osteoclastogenesis, rheumatoid arthritis, ACPA

Posted Date: April 17th, 2020

DOI: https://doi.org/10.21203/rs.3.rs-21873/v1

Abstract

Background. Anti-citrullinated protein/peptide antibodies (ACPA) play important roles in the pathogenesis of rheumatoid arthritis (RA), and are associated with RA severity. It has been suggested that ACPA-positive (ACPA+) and ACPA-negative (ACPA-) RA are different disease subsets with distinct differences in genetic variation and clinical outcomes. The aims of the present study were to compare gene expression profiles in ACPA + and ACPA- RA and identify novel candidate gene signatures that might serve as therapeutic targets.

Methods. Comprehensive transcriptome analysis of peripheral blood mononuclear cells (PBMCs) from ACPA + and ACPA- RA patients, and healthy controls was performed via RNA sequencing. Genes with significantly different expressions were analyzed by cluster analysis, Gene Ontology analysis and Ingenuity Pathway analysis. A validation cohort was used to further investigate differentially expressed genes via real-time PCR and enzyme-linked immunosorbent assay. Spearman's correlation test was used to evaluate the correlation of differentially expressed genes and the clinical and laboratory data of the patients. The role of differentially expressed genes in osteoclastogenesis was further investigated.

Results. There were significant differences in the expression levels of both genes and gene isoforms between ACPA + and ACPA- RA samples. Expression of C-X-C motif chemokine ligand 2 (CXCL2) was significantly increased in ACPA + RA patients than in ACPA- RA patients and healthy controls. Validation of candidate genes expression showed that CXCL2 levels in PBMCs and serum were higher in ACPA + RA patients than in ACPA- RA patients and healthy controls. CXCL2 promoted the migration of CD14 + monocytes and increased osteoclast differentiation in RA patients. RAW264.7 macrophages were used to investigate specific mechanisms, and the results suggested that CXCL2 stimulated osteoclastogenesis via ERK MAPK and NFκB pathways.

Conclusion. Novel pathways associated with ACPA + RA were identified via RNA sequencing, and CXCL2 was highly expressed in ACPA + RA than in ACPA- RA. These results reveal a previously unreported role of CXCL2 during osteoclastogenesis in RA, and suggest that the blockade of CXCL2 might be a novel strategy for the treatment of RA.

Introduction

Rheumatoid arthritis (RA) is a systemic autoimmune disease that involves activation of inflammatory cells, synovial hyperplasia, and destruction of cartilage and bone(1). In recent years, anti-citrullinated protein/peptide antibodies (ACPAs) have been used as biomarkers in the diagnosis of RA, and to predict clinical outcomes(2–4). Based on the presence or absence of ACPA, RA can be classified into two subtypes as ACPA-positive (ACPA+) or ACPA-negative (ACPA-). It has been reported that ACPAs are detectable years before the onset of arthritis, and they are strong predictors of progression to classic RA in patients with undifferentiated arthritis(5, 6). Moreover, ACPAs are associated with RA severity. RA patients with ACPAs exhibit more severe radiographic damage than those without ACPAs(7–10). Many

studies have suggested that ACPAs play a pathophysiologic role in RA(11). In recent years, a number of candidate genes have been shown to be differentially associated with susceptibility in ACPA + and ACPA- RA(12–14). With the advent of next-generation sequencing technologies such as RNA sequencing, more comprehensive and accurate transcriptome analysis has become feasible and affordable. In RNA sequencing, short fragments of complementary DNA (cDNA) are sequenced (‘reads’) then mapped onto the reference genome. RNA sequencing facilitates both the identification of differentially expressed genes and precise quantitative determination of exon and isoform (alternative splicing) expression, along with the characterisation of transcription initiation sites and new splicing variants(15, 16).

In the present study, comprehensive transcriptome analysis of PBMCs from ACPA + and ACPA- RA patients was performed to identify novel candidate gene signatures that might be involved in the pathogenesis of different subsets of disease.

Methods

Patients

Two ACPA+ and two ACPA- RA patients from Peking University Third Hospital who fulfilled the 2010 European League Against Rheumatism/American College of Rheumatology classification criteria for RA(2) were enrolled in the study. All 4 patients were newly diagnosed, treatment naive, menopausal, and non-smoker women from the northern Han population with symptom duration of less than 6 months, and none had any other chronic diseases. Three matched healthy individuals were included in the study.

PBMC collected from 40 ACPA+, 40 ACPA- RA patients, and 40 healthy controls were applied for quantitative PCR to validate candidate genes expression. Serum CXCL2 levels were detected by ELISA in a cohort consisted of 70 ACPA+, 37 ACPA- RA patients, and 40 healthy controls. The clinical and laboratory data of the patients were collected from electronic medical records. In all comparisons mentioned, the groups were age and sex matched. The present study was conducted in accordance with the Declaration of Helsinki. The Ethics Committee of Peking University Third Hospital approved the study. All procedures involving specimens obtained from humans were performed with informed consent from each patient.

RNA extraction, sequencing and analysis

PBMCs were isolated from the blood of RA patients and healthy donors via centrifugation over Ficoll-Paque Plus (GE Healthcare, Sweden). RNA was extracted from PBMCs using Trizol: chloroform, precipitated in isopropanol. Sample quality was assessed using Nanodrop. Total RNA was enriched for mRNA using poly-A selection. In brief, mRNA was fragmented, reverse transcribed, adapted with sequencing primers and sample barcodes, size selected, and PCR enriched. Libraries were sequenced on the HiSeq 2000 platform. RNA sequence reads were aligned to the human reference genome (NCBI, hg19) using TopHat2 aligners. Normalised gene counts were calculated using HTSeq, and differential gene expression between samples was identified via edgeR. Gene expression (RPKM) values were calculated

using Cufflinks v2.0.2. Gene Ontology (http://geneontology.org/) associations were determined using Gorilla. Network construction was based on the Ingenuity Pathway Analysis (Qiagen, CA, USA) experimental evidence database.

Cell culture

PBMCs were isolated from the blood of RA patients as described above. CD14+ monocytes were positively selected via magnetic-activated cell sorting (Miltenyi Biotec, Germany) and an anti-CD14 antibody. The isolated CD14+ monocytes (1.5×10^5 cells per well in 48-well plates or 6×10^5 cells per well in 12-well plates) were incubated in RPMI-1640 media containing 10% fetal bovine serum (FBS). Osteoclast differentiation was induced from CD14+ monocytes treated with macrophage colony-stimulating factor (M-CSF, 50 ng/ml) and receptor activator of nuclear factor kappa-B ligand (RANKL, 100 ng/ml). C-X-C motif chemokine ligand 2 (CXCL2, 100 ng/ml or otherwise as indicated) were added to the cultures. The medium was replaced every 3 days.

RAW264.7 macrophages (1.0×10^4 cells per well in 48-well plates or 4.5×10^4 cells per well in 12-well plates) were incubated in DMEM media containing 10% FBS. Osteoclast differentiation was induced by M-CSF (10 ng/ml) and RANKL (50 ng/ml) with or without CXCL2.

Flow cytometry

To identify the expression of C-X-C motif chemokine receptor 2 (CXCR2), CD14+ monocytes were incubated for 45 min at 4°C with anti-human CXCR2 in the dark. Cells were washed twice with staining wash buffer and centrifuged at 1000 rpm for 5 minutes to pellet the cells. Stained cells were resuspended in 200 µl of PBS then analyzed via flow cytometry. In each case, staining was compared with that of the appropriately labeled isotype control antibody.

Cell migration

Monocyte migration testing was performed with 5µm pore-size polycarbonate membrane transwell tissue culture inserts (Corning, USA). Cells (5×10^4 per well) were seeded into the wells in the top chamber in 10% FBS medium, and CXCL2 was added to the lower chamber in 10% FBS medium. After incubation for 1 hour at 37°C the medium was removed and the filters were fixed with 4% paraformaldehyde for 20 minutes. The filters were then stained with 0.1% crystal violet for 15 minutes. The number of cells that had migrated from the upper surface of the filter to the lower surface of the filter was counted.

Quantitative PCR

Total RNA was extracted using TRIzol reagent (Invitrogen), and 1 µg of total RNA was reverse-transcribed into cDNA using a FastQuant RT Kit (with gDNase) (Tiangen Biotech). RT-PCR was carried out using the QuantStudio™ 5 Real-Time PCR System (Thermo Fisher Scientific) with Talent qPCR PreMix (SYBR Green) (Tiangen Biotech). Data were normalized to the expression of GAPDH. The primer nucleotide sequences

for PCR were obtained from GenBank database and synthesized by Sangon Biotech (China). The primer sequence information used in the study was shown in the supplementary material, Table1.

Enzyme-linked immunosorbent assay

CXCL2 levels in sera from ACPA+ RA, ACPA- RA and healthy controls, as well as levels in the supernatants of CD14+ monocyte cultures were measured using human CXCL2 enzyme-linked immunosorbent assay kits in accordance with the manufacturer's instructions.

TRAP staining

TRAP staining of CD14+ monocytes and RAW264.7 macrophages was performed after culturing with or without CXCL2 in the presence of M-CSF and RANKL. TRAP staining was conducted using the TRAP kit (387A-1KT, Sigma) in accordance with the manufacturer's instructions. TRAP-positive multinucleated cells containing more than 3 nuclei were identified as osteoclasts and counted under a microscope.

F-actin ring immunofluorescence

Cells were fixed with 4% paraformaldehyde and incubated with FITC-conjugated anti-actin antibody for 1 hour at 25°C. After a PBS wash the cells were incubated with DAPI for 5 minutes at 25°C, then analyzed using an Olympus BX51 microscope (Tokyo, Japan).

Scanning electron microscopy

Cells on dentine were fixed in 4% glutaraldehyde, dehydrated via graded alcohol solutions then graded (50% to 100%) hexamethyldisilazane solutions (Sigma-Aldrich, MO, USA), then air-dried. Dentine slices were then mounted onto aluminium stubs (EMS, Hatfield, PA, USA), sputtered with gold, and examined using a scanning electron microscope (Philips SEM 505, Best, Netherlands).

Bone resorption assay

Functional evidence of osteoclast formation was determined via a lacunar resorption assay system using cell cultures on dentine slices as previously described(17). Cells were removed from the dentine slices by treatment with 0.1 M ammonium hydroxide. The dentine slices were washed in distilled water and ultrasonicated to remove adherent cells, then stained with 0.5% (v/v) toluidine blue to reveal areas of lacunar resorption, and examined via light microscopy.

Western blotting

Total protein was extracted using RIPA lysis buffer (Applygen, Beijing, China). A total of 40 μg of protein was loaded into a 10% sodium dodecyl sulphate-polyacrylamide gel and electrophoretically transferred to polyvinylidene fluoride membranes (Merck Millipore, Billerica, MA, USA). After blocking with 5% milk for 1 h, the membranes were incubated with specific antibodies at the indicated dilutions for 12–16 h at 4°C.

The membranes were scanned using an Odyssey Sa Imaging System (LICOR Biosciences, Lincoln, NE, USA). The antibody information used in this study was shown in the supplementary material, Table 2.

Statistical analysis

Statistical analysis of RNA sequencing count data was conducted using edgeR with a 5% FDR. All experiments were repeated at least three times and are presented as the mean±standard deviation and the median with interquartile range. Statistical analysis were assessed via Spearman correlation, Mann-Whitney test and one-way analysis of variance followed by Tukey's test for multiple comparisons. p values < 0.05 were considered statistically significant.

Results

Selection of candidate genes using RNA sequencing

Further analysis was conducted on RNA sequencing data from 7 samples; 2 ACPA+ RA patients, 2 ACPA- RA patients and 3 healthy controls. Differentially expressed genes (DEGs) were analyzed in the two different sample types, and three groups of DEGs were identified (ACPA+ vs. control, ACPA+ vs. ACPA-, ACPA- vs. control). We identified 1007 DEGs (522 up-regulated and 485 down-regulated) between ACPA+ and control, 628 DEGs (344 up-regulated and 284 down-regulated) between ACPA+ and ACPA-, and 1097 DEGs (549 up-regulated and 548 down-regulated) between ACPA- and control (Fig. 1A and 1B). All these DEGs exhibited distinct expression patterns in the three sample types (Fig. 1C).

Pathway enrichment analysis/ingenuity pathway analysis of DEGs yielded 19 canonical pathways that were significantly enriched between ACPA+ and control, 24 between ACPA+ and ACPA-, and 35 between ACPA- and control (see supplementary information). Some of these pathways were enriched in more than one comparison (Fig. 1D). The agranulocyte adhesion and diapedesis pathway was particularly enriched in ACPA+ vs. control and ACPA+ vs. ACPA- (Fig. 1D). Different DEGs were involved in the agranulocyte adhesion and diapedesis pathway in two comparisons (Fig. 1E and 1F), and of these, CXCL2 and C-X-C motif chemokine ligand 7 (CXCL7) were exclusively up-regulated in ACPA+ samples (Fig. 1E).

Validation of candidate genes expression in ACPA+ RA patients

To validate the differential expression levels of candidate genes in ACPA+ and ACPA- RA patients, the expression levels of CXCL2 and CXCL7 were measured using real time PCR. CXCL2 levels were higher in ACPA+ RA patients (n=40) than in ACPA- RA patients (n=40) and healthy controls (n=40) (Fig. 2A), confirming that CXCL2 was differentially expressed in ACPA+ RA patients and ACPA- RA patients. However, there was no significant difference in CXCL7 expression between ACPA+ RA patients and ACPA- RA patients.

CXCL2 levels in serum and CD14+ cell supernatant

CXCL2 levels in sera were detected in 70 ACPA+ RA patients, 37 ACPA- RA patients and 40 healthy controls. Age and sex were balanced between the groups, whereas the disease duration, RF positive rate and bone erosion positive rate were significantly different among ACPA+ RA patients and ACPA- RA patients (Table 1).

Median serum CXCL2 in RA patients (1083.43, (586.94,1569.50) pg/ml) was significantly higher than in healthy controls (301.44, (217.62,422.26) pg/ml) ($p < 0.001$; Fig, 2B). And median serum CXCL2 was significantly higher in ACPA+ RA patients than in ACPA- RA patients ($p < 0.05$; Fig. 2C). Correlation analysis showed that CXCL2 was positively correlated with DAS28 ($r=0.4594$, $p < 0.001$), ESR ($r=0.3985$, $p <0.001$) and CRP ($r=0.3726$, $p < 0.001$) (Fig. 2D). However, the CXCL2 level was not related to disease duration ($r=-0.084$, $p=0.391$) and RF titer ($r=0.1358$, $p=0.309$). Serum CXCL2 was significantly higher in RA patients with bone erosion than in RA patients without bone erosion ($p < 0.05$; Fig. 2E).

CXCL2 expression was significantly higher in the supernatant of CD14+ monocyte cultures derived from ACPA+ RA patients than from the ACPA- RA patients (Fig. 2F).

CXCL2 promoted migration of CD14+ monocytes from RA patients

Flow cytometry analysis using anti-CXCR2 antibody revealed that CD14+ monocytes from ACPA+ patients expressed CXCR2 at a higher level than those from ACPA- patients, but the difference was not statistically significant (Fig. 3A). In the transwell experiments, CXCL2 significantly increased the number of migrating monocytes in cultures derived from RA patients (Fig. 3B).

CXCL2 increased osteoclast differentiation and enhanced osteoclastic bone resorption

In experiments conducted to evaluate the effects of CXCL2 on osteoclastogenesis, cultures from all groups formed osteoclasts on plastic and the average numbers of osteoclasts were similar in the control cultures and cultures exposed to a low concentration of CXCL2 (10 ng/mL). However, high doses of CXCL2 tended to promote the formation of osteoclasts (Fig. 4A). Formation of the F-actin ring by osteoclasts is a necessary step in bone resorption. Immunofluorescence microscopy of CD14+ monocytes cultured for 14 days treated with CXCL2 (100 ng/ml) in the presence of M-CSF and RANKL revealed that F-actin rings were significantly increased in number (Fig. 4B). CXCL2 stimulation also increased cell fusion, resulting in multinucleated cells (Fig. 4C), which suggested that CXCL2 promoted osteoclast formation.

Functional evidence of osteoclast formation was obtained via the lacunar resorption assay system using cell cultures on dentine slices. The result showed that the resorption area was increased in bone slices exposed to CXCL2 (Fig. 4D). Expression of the osteoclast markers RANK, cathepsin K, and TRAP was significantly increased after 3 days of stimulation with the CXCL2 (100 ng/mL) in the presence of M-CSF (50 ng/ml) and RANKL (100 ng/ml) ($p < 0.05$; Fig. 4E).

Consistent with the results obtained in CD14+ monocytes, the effects of exogenous CXCL2 on osteoclast formation were also observed in RAW264.7 cells. Compared with the control group, much larger

multinucleated cells were evident in the CXCL2 groups (Fig. 5A). Expression of osteoclast markers such as cathepsin K and TRAP was also significantly increased in the CXCL2 group after 3 days of stimulation in the presence of M-CSF and RANKL ($p < 0.05$; Fig. 5B). These results suggest that CXCL2 enhances osteoclast formation and bone resorption. In addition, CXCL2 significantly increased the expression of NFATc1 and c-Fos by RAW264.7 cells after 5 days of stimulation with M-CSF (10 ng/ml) and RANKL (50 ng/ml) ($p < 0.05$; Fig. 5C).

CXCL2 stimulated osteoclastogenesis via ERK MAPK and NFκB pathways

To explore the signal pathways involved in the osteoclastogenesis with the stimulation of CXCL2, RAW264.7 cells were incubated in osteoclast-promoting medium with or without CXCL2, western blotting at different time-points was conducted to detect the phosphorylation of IκBα, p65, ERK1/2 and JNK. The addition of CXCL2 dramatically promoted phosphorylation of p65 and ERK1/2 (Fig. 6A, B), with no effect on the phosphorylation of IκBα or JNK (Fig. 6C, D).

Discussion

RNA sequencing technology has been used to detect differences in gene expression profiles in RA patients for the last few years. Several gene expression profiling studies of synovial tissues and PBMCs from RA patients have revealed marked variation in gene expression profiles that have facilitated the identification of distinct molecular disease mechanisms involved in RA pathology(18–21). The heterogeneity of RA was demonstrated by the presence of distinct autoantibody specificities such as ACPA in serum, differential responsiveness to treatment, and variability in clinical presentation. RA patients can be stratified into two subgroups defined by the presence or absence of ACPA, and ACPA + patients exhibit more severe inflammation and radiographic damage than ACPA- patients(5–7). In the present study, various genes were compared in ACPA + and ACPA- patients via RNA sequencing, and two significantly increased chemokines, CXCL2 and CXCL7 were identified in ACPA + patients. The next more focused analysis using PCR technology on many more patients found that only CXCL2 was differentially expressed in ACPA + RA patients and ACPA-RA patients. There was no significant difference in CXCL7 expression between ACPA + RA patients and ACPA- RA patients.

CXCL2 was first identified as a major chemokine produced by endotoxin-treated macrophages(22), which bind to the G-protein coupled receptor CXCR2 expressed on macrophages, neutrophils, and epithelial cells(23). In previous studies, CXCL2 level was found to be higher expressed in RA patients than in normal controls(24). Xiaokun *et al*. downloaded microarray datasets of GSE1919, GSE12021, and GSE21959 (35 RA samples and 32 normal controls) from the Gene Expression Omnibus database (https://www.ncbi.nlm.nih.gov/geo/) and identified DEGs in RA samples. They found that CXCL2 was strongly associated with DEGs involved in RA progression(24). Jacobs *et al*.(25) performed a microarray analysis to characterize the molecular events underlying pathology in autoantibody-mediated arthritis and reported that CXCL2 was up-regulated in parallel with the disease. Jeongim *et al*.(26) reported that CXCL2 was significantly higher in synovial fluid and sera from RA patients compared with corresponding

samples from osteoarthritis patients. In the present study, serum CXCL2 was significantly increased in RA patients compared with healthy controls, and serum CXCL2 was higher in ACPA + RA patients than in ACPA- RA patients. Compared with ACPA − patients, ACPA + patients had longer disease duration and higher positive rate of RF. To exclude the impact of these two factors on CXCL2 level, correlation analysis was applied and showed that CXCL2 was irrelevant to disease duration and RF titer.

CXCL2 was involved in various biological progresses, such as angiogenesis, inflammation and cancer biological behaviors(23, 27–30). CXCL2 was also considered to be a proinflammatory factor in RA(24). In line with this, our study showed that CXCL2 was positively correlated with DAS28, ESR and CRP. Moreover, recent studies revealed CXCL2 was also involved in the process of osteoclastogenesis(26, 31). In the present study, we also found serum CXCL2 was significantly higher in RA patients with bone erosion than in RA patients without bone erosion. Thus, we hypothesized that CXCL2 could be one of the key molecules upregulated in RA progression, especially in ACPA + RA which exhibit more radiographic damage, and focused on the CXCL2 for subsequent analyses.

As the most important osteoclast precursors, CD14 + monocytes were derived from ACPA + patients and exhibited elevated CXCL2 secretion compared with those derived from ACPA- patients. CXCR2 is known to be the major receptor for CXCL2(32). It has been suggested that CXCL2 acts as a chemoattractant for various types of cells by binding to CXCR2, and monocytes constitutively express CXCR2(32). However, whether there is a difference in the expression of cell surface CXCR2 in CD14 + monocytes from ACPA + and ACPA- RA patients remains unclear. In the present study, we found that CXCR2 expression was higher on the surfaces of CD14 + monocytes derived from ACPA + patients than those from ACPA- patients, but the difference was not statistically significant.

ACPA + RA patients usually develop more severe radiological damage, and enhanced osteoclastogenesis may be involved in the bone erosion(7). Osteoclasts are polykaryocytes formed via the fusion of mononuclear monocytic precursors such as monocytes in peripheral blood. We surmise that elevated CXCL2 may recruit more monocytes to joint sites and augment the formation of osteoclasts. The present study showed that CXCL2 promoted the migration, differentiation, and function of osteoclasts in experiments using CD14 + monocytes isolated from RA patients.

The effects of CXCL2 on activating the signaling pathway during osteoclast differentiation were examined to explore the molecular mechanisms of the observed enhancement effect on osteoclastogenesis. The addition of CXCL2 resulted in dramatically increased phosphorylation of p65 and ERK1/2, while it did not affect the phosphorylation of IκBα or JNK. NFATc1 and c-Fos are critical transcription factors in the regulation of osteoclast differentiation(33). In the current study, NFATc1 and c-fos were increased significantly with stimulation of CXCL2 in the presence of M-CSF and RANKL. NFATc1 is an important regulatory factor in the process of osteoclast differentiation mediated by RANKL-activated MAPK and NFκB signalling pathways(34). Therefore, it suggests that CXCL2 may promote osteoclast differentiation and bone resorption by regulating NFATc1 expression via interfering with the phosphorylation of NFκB p65 and MAPK ERK1/2.

Jeongim *et al.*(26) reported that RANKL significantly increased the expression of CXCL2 in bone marrow-derived macrophages (BMMs) and that CXCL2 mediated RANKL-dependent differentiation of osteoclasts from BMMs in mice. The osteoclastogenesis-enhancing effects of CXCL2 were further corroborated by their investigation with an in vivo bone resorption model. Notably, CXCL2 alone induced significant bone loss in mice calvarial similar to that induced by RANKL. They also reported that CXCL2 mediated lipopolysaccharide (LPS)-induced osteoclastogenesis in RANKL-primed precursors (i.e. BMMs) (31). LPS stimulated the production of CXCL2 in BMMs, and the conditioned medium from LPS-treated BMMs could enhance the migration of osteoclast precursors, which was blocked by treatment with CXCL2-neutralising antibody or CXCR2 receptor antagonist. Blocking CXCL2 also reduced LPS-induced osteoclastogenesis, and in addition, CXCL2 neutralization prevented bone destruction in mice treated with LPS, suggesting a critical role of CXCL2 in the process of osteoclastogenesis. In the present study, CXCL2 was also evidently involved in the process of osteoclast differentiation in RA patients.

Therapies targeting CXCL2/CXCR2 have been tested in animal models of arthritis with concomitant reduction in neutrophil recruitment and tumor necrosis factor-α production(35, 36), and immunization against CXCL2 was reportedly efficient in delaying the onset of arthritis and reducing disease severity in a murine collagen-induced arthritis model(37). The novel orally-active non-competitive allosteric inhibitor of CXCL2 known as DF 2162 significantly ameliorates AIA in rats, an effect that is quantitatively and qualitatively similar to that of anti-tumor necrosis factor antibody treatment(35). In addition, the CXCR2 antagonist SCH563705 led to a dose-dependent decrease in clinical disease scores and paw thickness measurements, and clearly reduced inflammation and bone and cartilage degradation in a mouse model of arthritis(36). The results of our study imply that targeting CXCL2/CXCR2 as a strategy to treat RA may contribute to protection from bone destruction by directly inhibiting bone resorption, in addition to the already suggested anti-inflammatory effects.

Conclusion

In conclusion, we identified novel pathways associated with ACPA + RA patients using RNA sequencing, and detected higher CXCL2 expression in ACPA + RA patients than in ACPA- RA patients. Increased levels of CXCL2 led to NFκB activation in CD14 + monocytes from RA patients during the osteoclastogenic process. These results suggest a previously unreported role of CXCL2 during osteoclastogenesis in RA patients, and indicate that CXCL2 blockade might be a novel therapeutic strategy in RA.

Abbreviations

ACPA: Anti-citrullinated protein/peptide antibodies; CXCL2: C-X-C motif chemokine ligand 2; CXCL7: C-X-C motif chemokine ligand 7; CXCR2: C-X-C motif chemokine receptor 2; DEGs: Differentially expressed genes; M-CSF: Macrophage colony-stimulating factor; PBMCs: Peripheral blood mononuclear cells; RANKL: Receptor activator of nuclear factor kappa-B ligand; RA: Rheumatoid arthritis

Declarations

Acknowledgements

We gratefully thank the Medical Research Center of Peking University Third Hospital for providing experimental equipment and technical support.

Authors' contributions

LS, XW, NH, ZA, RY, YL, YL and XL carried out the molecular biochemical studies. LS, XW and NH drafted the manuscript and performed the statistical analysis. XF and JZ participated in the design of the study and helped to draft manuscript. All authors read and approved the final manuscript.

Funding

This work was supported by the National Natural Science Foundation of China (No.81571573 and No. 81771744).

Availability of data and materials

Not applicable.

Ethics approval and consent to participate

This study was approved by Ethics Committee of Peking University Third Hospital (IRB00006761-2015044). All patients and controls participated in this study provided written informed consent.

Consent for publication

Not applicable.

Competing interests

The authors declare no conflicts of interest.

References

1. Li R, Sun J, Ren LM, Wang HY, Liu WH, Zhang XW, et al. Epidemiology of eight common rheumatic diseases in China: a large-scale cross-sectional survey in Beijing. Rheumatology. 2012;51(4):721–9.
2. Aletaha D, Neogi T, Silman AJ, Funovits J, Felson DT, Bingham CO 3. 2010 Rheumatoid arthritis classification criteria: an American College of Rheumatology/European League Against Rheumatism collaborative initiative. Arthritis rheumatism. 2010;62(9):2569–81. rd, et al.
3. Zhao J, Su Y, Li R, Ye H, Zou Q, Fang Y, et al. Classification criteria of early rheumatoid arthritis and validation of its performance in a multi-centre cohort. Clin Exp Rheumatol. 2014;32(5):667–73.
4. Burgers LE, van Steenbergen HW, Ten Brinck RM, Huizinga TW, van der Helm-van Mil AH. Differences in the symptomatic phase preceding ACPA-positive and ACPA-negative RA: a longitudinal study in

arthralgia during progression to clinical arthritis. Ann Rheum Dis. 2017;76(10):1751–4.

5. Ding B, Padyukov L, Lundstrom E, Seielstad M, Plenge RM, Oksenberg JR, et al. Different patterns of associations with anti-citrullinated protein antibody-positive and anti-citrullinated protein antibody-negative rheumatoid arthritis in the extended major histocompatibility complex region. Arthritis rheumatism. 2009;60(1):30–8.
6. Belakova G, Manka V, Zanova E, Racay P. Benefits of anticitrullinated peptides examination in rheumatoid arthritis. Niger J Clin Pract. 2018;21(10):1380–3.
7. Im CH, Kang EH, Ryu HJ, Lee JH, Lee EY, Lee YJ, et al. Anti-cyclic citrullinated peptide antibody is associated with radiographic erosion in rheumatoid arthritis independently of shared epitope status. Rheumatol Int. 2009;29(3):251–6.
8. Cheng TT, Yu SF, Su FM, Chen YC, Su BY, Chiu WC, et al. Anti-CCP-positive patients with RA have a higher 10-year probability of fracture evaluated by FRAX(R): a registry study of RA with osteoporosis/fracture. Arthritis research therapy. 2018;20(1):16.
9. Hecht C, Englbrecht M, Rech J, Schmidt S, Araujo E, Engelke K, et al. Additive effect of anti-citrullinated protein antibodies and rheumatoid factor on bone erosions in patients with RA. Ann Rheum Dis. 2015;74(12):2151–6.
10. Schett G. The role of ACPAs in at-risk individuals: Early targeting of the bone and joints. Best practice research Clinical rheumatology. 2017;31(1):53–8.
11. England BR, Thiele GM, Mikuls TR. Anticitrullinated protein antibodies: origin and role in the pathogenesis of rheumatoid arthritis. Curr Opin Rheumatol. 2017;29(1):57–64.
12. Padyukov L, Seielstad M, Ong RT, Ding B, Ronnelid J, Seddighzadeh M, et al. A genome-wide association study suggests contrasting associations in ACPA-positive versus ACPA-negative rheumatoid arthritis. Ann Rheum Dis. 2011;70(2):259–65.
13. Viatte S, Plant D, Bowes J, Lunt M, Eyre S, Barton A, et al. Genetic markers of rheumatoid arthritis susceptibility in anti-citrullinated peptide antibody negative patients. Ann Rheum Dis. 2012;71(12):1984–90.
14. Yarwood A, Huizinga TW, Worthington J. The genetics of rheumatoid arthritis: risk and protection in different stages of the evolution of RA. Rheumatology. 2016;55(2):199–209.
15. Marioni JC, Mason CE, Mane SM, Stephens M, Gilad Y. RNA-seq: an assessment of technical reproducibility and comparison with gene expression arrays. Genome research. 2008;18(9):1509–17.
16. Heruth DP, Gibson M, Grigoryev DN, Zhang LQ, Ye SQ. RNA-seq analysis of synovial fibroblasts brings new insights into rheumatoid arthritis. Cell bioscience. 2012;2(1):43.
17. Adamopoulos IE, Chao CC, Geissler R, Laface D, Blumenschein W, Iwakura Y, et al. Interleukin-17A upregulates receptor activator of NF-kappaB on osteoclast precursors. Arthritis research therapy. 2010;12(1):R29.
18. Pratt AG, Swan DC, Richardson S, Wilson G, Hilkens CM, Young DA, et al. A CD4 T cell gene signature for early rheumatoid arthritis implicates interleukin 6-mediated STAT3 signalling, particularly in anti-citrullinated peptide antibody-negative disease. Ann Rheum Dis. 2012;71(8):1374–81.

19. Wright HL, Cox T, Moots RJ, Edwards SW. Neutrophil biomarkers predict response to therapy with tumor necrosis factor inhibitors in rheumatoid arthritis. J Leukoc Biol. 2017;101(3):785–95.
20. Yu F, Duan C, Zhang X, Yao D, Si G, Gao Y, et al. RNA-seq analysis reveals different gene ontologies and pathways in rheumatoid arthritis and Kashin-Beck disease. Int J Rheum Dis. 2018;21(9):1686–94.
21. Sumitomo S, Nagafuchi Y, Tsuchida Y, Tsuchiya H, Ota M, Ishigaki K, et al. Transcriptome analysis of peripheral blood from patients with rheumatoid arthritis: a systematic review. Inflammation regeneration. 2018;38:21.
22. Wolpe SD, Cerami A. Macrophage inflammatory proteins 1 and 2: members of a novel superfamily of cytokines. FASEB J. 1989;3(14):2565–73.
23. De Filippo K, Dudeck A, Hasenberg M, Nye E, van Rooijen N, Hartmann K, et al. Mast cell and macrophage chemokines CXCL1/CXCL2 control the early stage of neutrophil recruitment during tissue inflammation. Blood. 2013;121(24):4930–7.
24. Gang X, Sun Y, Li F, Yu T, Jiang Z, Zhu X, et al. Identification of key genes associated with rheumatoid arthritis with bioinformatics approach. Medicine. 2017;96(31):e7673.
25. Jacobs JP, Ortiz-Lopez A, Campbell JJ, Gerard CJ, Mathis D, Benoist C. Deficiency of CXCR2, but not other chemokine receptors, attenuates autoantibody-mediated arthritis in a murine model. Arthritis rheumatism. 2010;62(7):1921–32.
26. Ha J, Choi HS, Lee Y, Kwon HJ, Song YW, Kim HH. CXC chemokine ligand 2 induced by receptor activator of NF-kappa B ligand enhances osteoclastogenesis. Journal of immunology (Baltimore, Md: 1950). 2010;184(9):4717-24.
27. Boro M, Balaji KN. CXCL1 and CXCL2 Regulate NLRP3 Inflammasome Activation via G-Protein-Coupled Receptor CXCR2. Journal of immunology (Baltimore, Md: 1950). 2017;199(5):1660-71.
28. Henn D, Abu-Halima M, Wermke D, Falkner F, Thomas B, Kopple C, et al. MicroRNA-regulated pathways of flow-stimulated angiogenesis and vascular remodeling in vivo. Journal of translational medicine. 2019;17(1):22.
29. Subat S, Mogushi K, Yasen M, Kohda T, Ishikawa Y, Tanaka H. Identification of genes and pathways, including the CXCL2 axis, altered by DNA methylation in hepatocellular carcinoma. J Cancer Res Clin Oncol. 2019;145(3):675–84.
30. Lu J, Xu W, Qian J, Wang S, Zhang B, Zhang L, et al. Transcriptome profiling analysis reveals that CXCL2 is involved in anlotinib resistance in human lung cancer cells. BMC Med Genom. 2019;12(Suppl 2):38.
31. Ha J, Lee Y, Kim HH. CXCL2 mediates lipopolysaccharide-induced osteoclastogenesis in RANKL-primed precursors. Cytokine. 2011;55(1):48–55.
32. Cheng Y, Ma XL, Wei YQ, Wei XW. Potential roles and targeted therapy of the CXCLs/CXCR2 axis in cancer and inflammatory diseases. Biochim Biophys Acta Rev Cancer. 2019;1871(2):289–312.
33. Park JH, Lee NK, Lee SY. Current Understanding of RANK Signaling in Osteoclast Differentiation and Maturation. Mol Cells. 2017;40(10):706–13.

34. Song F, Zhou L, Zhao J, Liu Q, Yang M, Tan R, et al. Eriodictyol Inhibits RANKL-Induced Osteoclast Formation and Function Via Inhibition of NFATc1 Activity. Journal of cellular physiology. 2016;231(9):1983–93.
35. Barsante MM, Cunha TM, Allegretti M, Cattani F, Policani F, Bizzarri C, et al. Blockade of the chemokine receptor CXCR2 ameliorates adjuvant-induced arthritis in rats. Br J Pharmacol. 2008;153(5):992–1002.
36. Min SH, Wang Y, Gonsiorek W, Anilkumar G, Kozlowski J, Lundell D, et al. Pharmacological targeting reveals distinct roles for CXCR2/CXCR1 and CCR2 in a mouse model of arthritis. Biochem Biophys Res Commun. 2010;391(1):1080–6.
37. Kim SJ, Chen Z, Essani AB, Elshabrawy HA, Volin MV, Fantuzzi G, et al. Differential impact of obesity on the pathogenesis of RA or preclinical models is contingent on the disease status. Ann Rheum Dis. 2017;76(4):731–9.

Table 1

Table 1 Baseline characteristics of the enrolled RA patients

	Total (n=107)	ACPA + (n=70)	ACPA – (n=37)	P Value
Age (mean year)	55.94±14.11	55.13±13.64	57.49±15.02	0.414
Gender (male/female)	26/81	16/54	10/27	0.632
Duration (months)	24 (12,108)	60 (17,183)	13 (5,36)	0.000
RF-positive	57.94%	82.86%	10.81%	0.000
ESR (mm/h)	32 (14,60)	33 (14.5,60)	29 (13.5,57.5)	0.692
CRP (mg/dl)	1.86 (0.51,5.22)	1.565 (0.5,4.37)	2.46 (0.61,7.72)	0.250
DAS28	5.84 (4.41,7.59)	6.62 (4.13,7.77)	5.64 (4.5,6.71)	0.187
Bone erosion	28.95% (n=22/76)	38% (n=19/50)	11.54% (n=3/26)	0.016

Data are represented as mean ± SD and median with interquartile range.

Figures

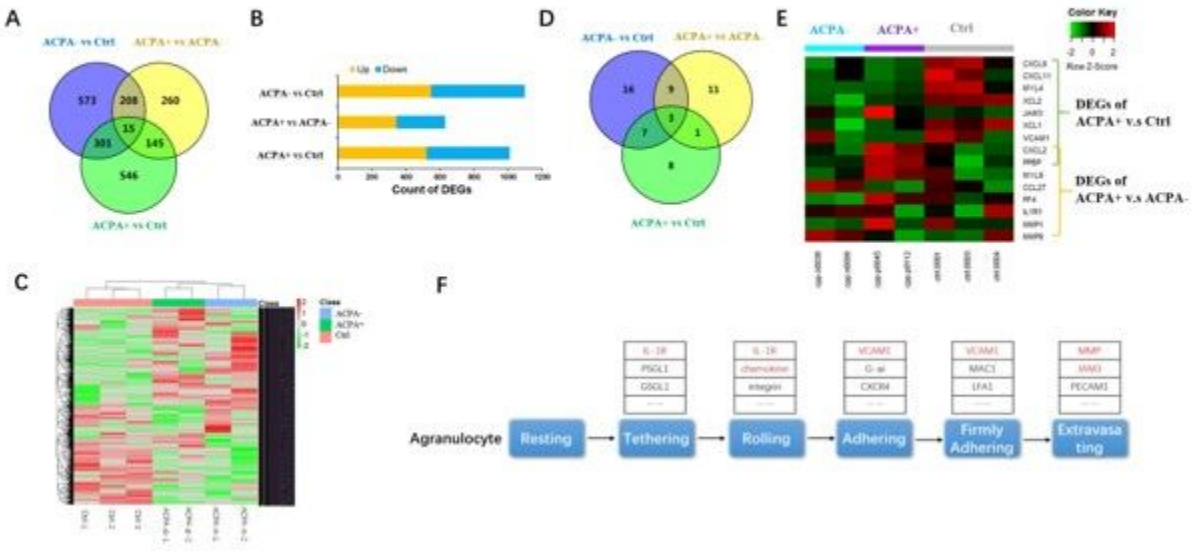

Figure 1

Transcriptome analysis of ACPA- RA patients (n=2), ACPA+ RA patients (n=2) and control (n=3) samples revealed the global gene expression pattern and identified Agranulocyte Adhesion and Diapedesis as one key pathway that particularizes ACPA+ RA. (A) Three groups of differentially expressed genes (DEGs) were identified using DEseq2 at a threshold of p-value < 0.05 Fold Change >2, the Venn diagram shows the overlap of three groups of DEGs. (B) Count of up-regulated and down-regulated genes. (C) Heat map of expression pattern of all 2048 DEGs in patient and control samples. (D) Each group of DEGs were submitted to pathway enrichment analysis using IPA, the Venn diagram shows the overlap of significantly enriched canonical pathways. Agranulocyte Adhesion and Diapedesis pathway significantly enriched in both ACPA+ v.s Ctrl group and ACPA+ v.s ACPA- group, but not in ACPA- v.s Ctrl group. (E) The heat map presents the expression pattern of DEGs that involve in Agranulocyte Adhesion and Diapedesis pathway. (F) A simplified schematic of Agranulocyte Adhesion and Diapedesis pathway and some involved genes, red marked genes are differentially expressed in ACPA+ RA patients.

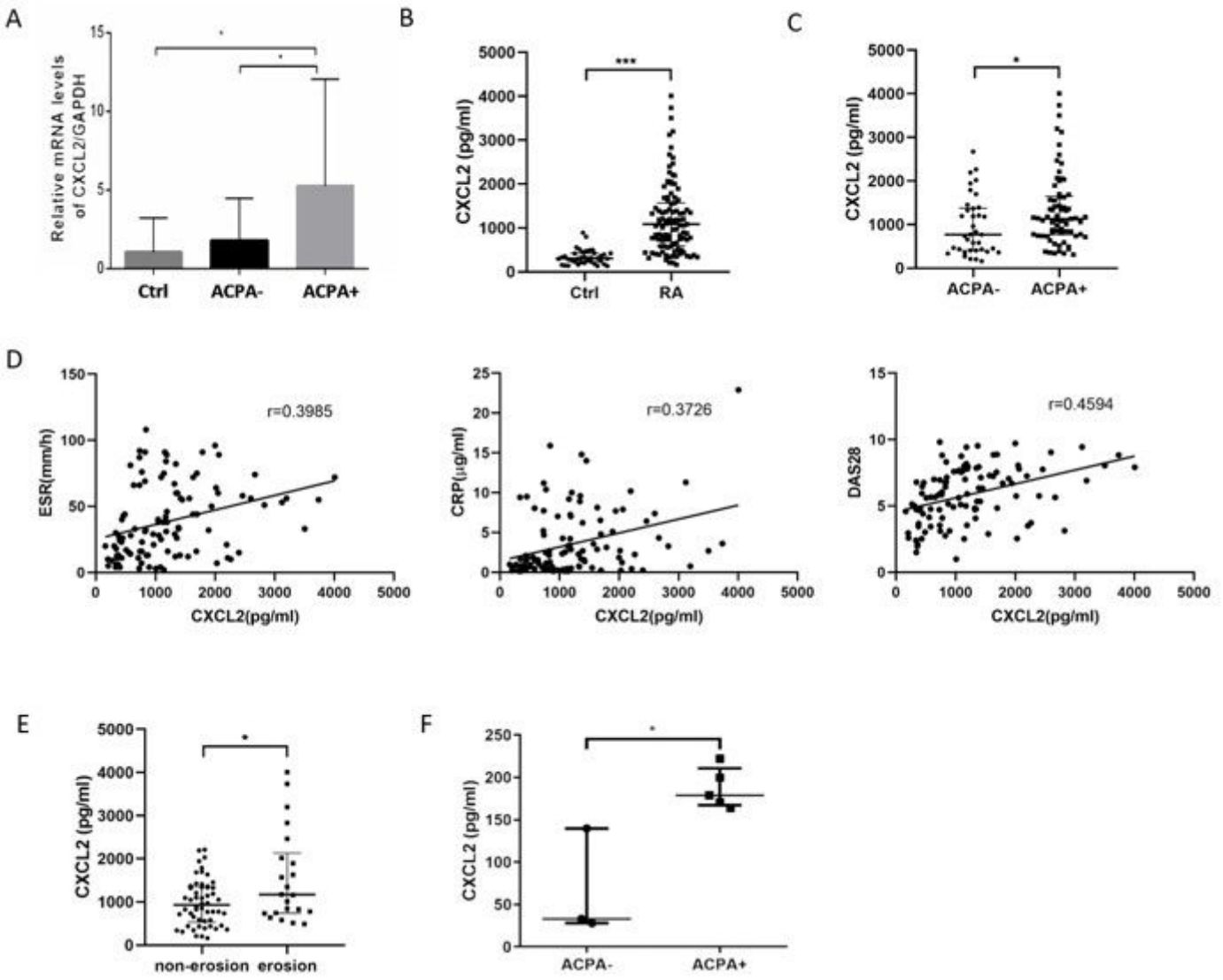

Figure 2

The expression of CXCL2 in RA patients (ACPA+, ACPA-) and control samples revealed higher CXCL2 expression in PBMC, serum and monocytes from ACPA+ RA patients. A. Validation of CXCL2 expression in PBMC from ACPA+ (n=40) RA patients, ACPA- (n=40) RA patients and normal controls (n=40) by real-time PCR. B. CXCL2 levels in sera of RA patients (n=107) and normal controls (n=40). C. The serum CXCL2 in ACPA+ (n=70) and ACPA- (n=37) RA patients. D. Correlations between CXCL2 and clinical parameters. E. CXCL2 levels in sera of RA patients without bone erosion (n=54) and patients with bone erosion (n=22). F. CXCL2 in the supernatant of CD14+ monocytes derived from ACPA+ (n=5) and ACPA- (n=3) RA patients. Data are expressed as mean ± SD (A) and median with interquartile range (B, C, E and F). *P < 0.05, **P < 0.01, ***P < 0.001.

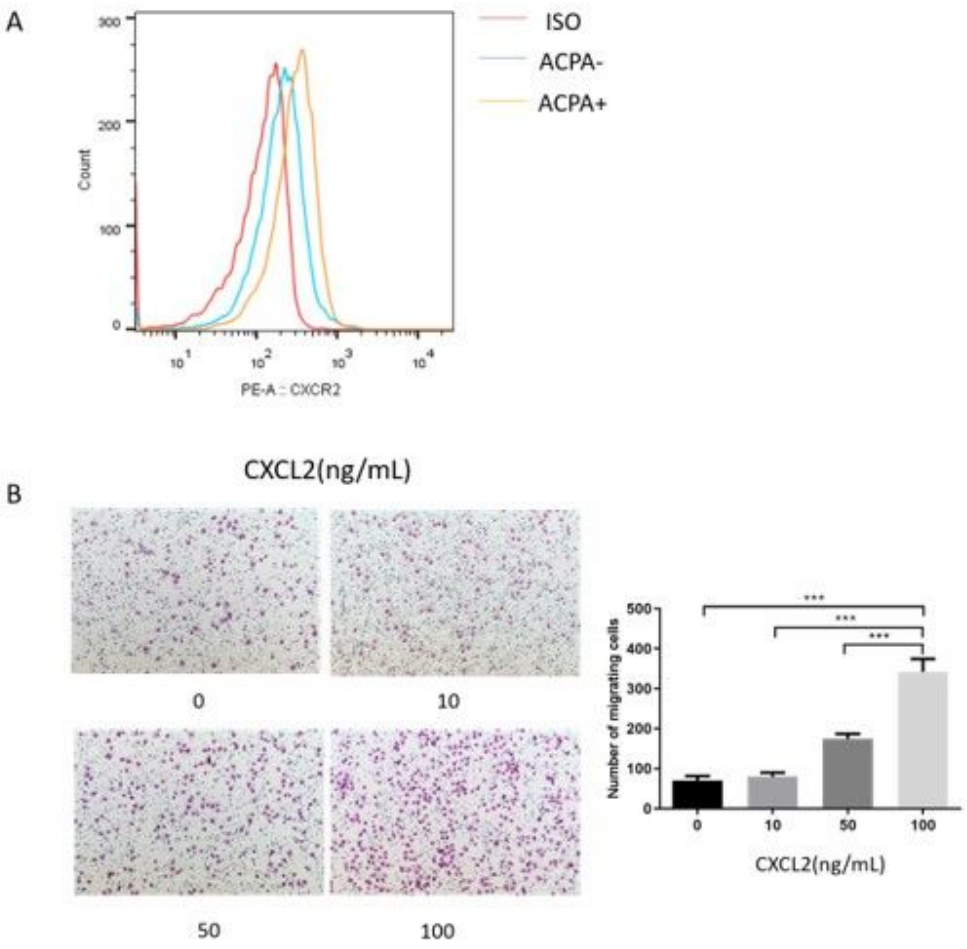

Figure 3

Migration of CD14+ monocytes from RA patients by CXCL2. A. The expression of CXCR2 on the surface of CD14+ monocytes isolated from ACPA+RA patients and ACPA-RA patients was analyzed by flow cytometry. B. A migration assay of CD14+ monocytes from RA patients was performed using the transwell system. The number of cells that migrated through to the lower surface was counted. n = 3 per group. Data are expressed as mean ± SD. ***P < 0.001.

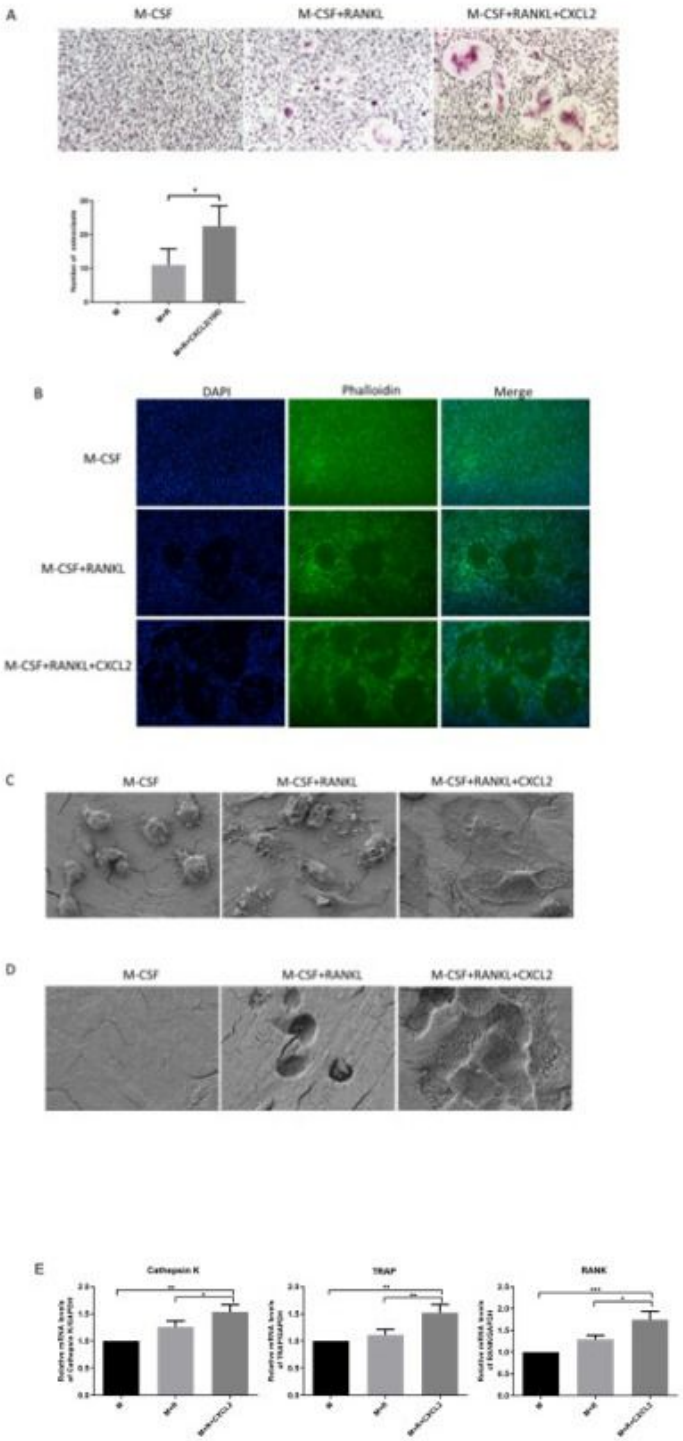

Figure 4

CXCL2 induced osteoclast differentiation and bone resorption. CD14+ monocytes isolated from RA patients were cultured in the presence of M-CSF (10 ng/ml) and RANKL (50 ng/ml) with CXCL2 (100ng/ml) during the osteoclastogenesis. A. Cells were then fixed with 4% paraformaldehyde and stained for tartrate-resistant acid phosphatase (TRAP). B. Cells were fixed and stained for F-actin. C. Representative scanning electron microscopy images of cell fusion. D. Representative scanning electron

microscopy images of bone resorption pits. E. CXCL2 increased the mRNA expression of cathepsin K, TRAP, and RANK. Three separate experiments were performed with similar results. Data are expressed as mean ± SD. *P < 0.05, **P < 0.01, ***P < 0.001.

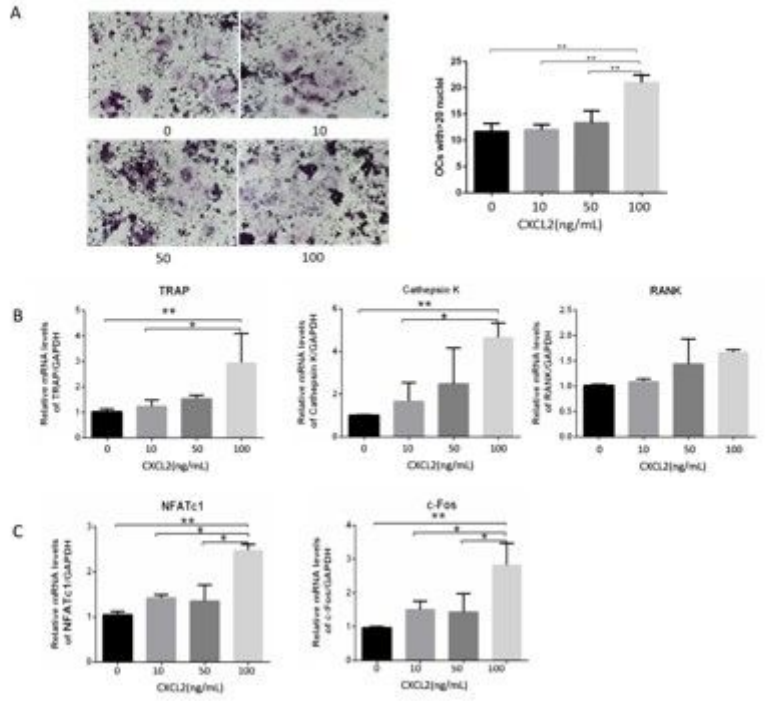

Figure 5

CXCL2 induced osteoclast differentiation in RAW264.7 cells. A. RAW264.7 cells were used to induce osteoclast formation for 5 days in M-CSF (10 ng/ml) and RANKL (50 ng/ml) with CXCL2. Large osteoclasts with more than 20 nuclei were counted. B. CXCL2 increased the mRNA expression of cathepsin K and TRAP at 3 days in RAW264.7 cells. C. CXCL2 induced the mRNA expression of NFATc1 and c-fos in RAW264.7 cells at 3 days in the presence of M-CSF and RANKL. Values shown were the mean ± SD for three separate experiments. *P < 0.05, **P < 0.01.

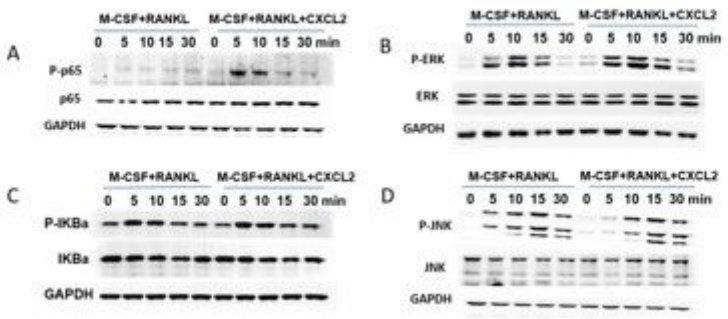

Figure 6

CXCL2 stimulated osteoclastogenesis through NF-kB p65 and MAPK ERK1/2 pathways in RAW264.7 cells. RAW264.7 cells were incubated in M-CSF and RANKL with or without CXCL2 (100ng/mL). A. CXCL2 increased the activation of the p-p65 at 5 and 10 min. B. CXCL2 increased the activation of the p-ERK at 5, 10 and 15 min. C. CXCL2 had no effect on the phosphorylation of IKBa. D. CXCL2 had no effect on the phosphorylation of JNK. Results are from one of three independent experiments.

Supplementary Files

This is a list of supplementary files associated with this preprint. Click to download.

- supplementarymaterial.docx